Pakistan J. Zool., pp 1-7, 2022. **DOI**: https://dx.doi.org/10.17582/journal.pjz/20220926100938

The Establishment and Evaluation of an Atherosclerotic Vulnerable Plaque Model Involving New Zealand Rabbits

Wenxiao Jia[1]*, Yilinuer Yilihamu[1], Yunling Wang[1], Shuang Ding[1], Dilinuerkezi Aihemaiti[1], Hanjiaerbieke Kukun[1] and Yanhui Ning[2]

[1]*Department of Radiology, First Affiliated Hospital of Xinjiang Medical University, Urumqi 830011, China*
[2]*Xinjiang Kangzhirui Biomedical Technology Service Company, Urumqi 830001, China*

Article Information
Received 26 September 2022
Revised 15 October 2022
Accepted 22 November 2022
Available online 30 January 2023
(early access)

Authors' Contribution
JWX and YY conception and design of the research. JWX, YY and WYL acquisition of data. YY, DS, DA and HK analysis and interpretation of the data. JWX, YY, WYL, DA, DS, HK and NYH statistical analysis, obtaining financing. YY and JWX writing of the manuscript. JWX critical revision of the manuscript for intellectual content.

Key words
Atherosclerotic vulnerable plaque, Animal model, Balloon injury, New Zealand rabbits, Abdominal aorta

ABSTRACT

This study aims to explore the feasibility of a new combined method of constructing an unstable atherosclerotic plaque model in the abdominal aorta of New Zealand rabbits. The experimental New Zealand rabbits were fed adaptively for one week before being punctured through the abdominal aorta with a balloon to injure the intima. Vitamin D (1.5 mL/kg) was administered one week after the surgical model was completed. Following injection, the animals were fed a high-fat diet for 16 weeks. High-resolution magnetic resonance imaging (HR-MRI) and a histology-based method were used to examine the abdominal aortic lesions. The overall mortality rate of the New Zealand rabbit model of unstable atherosclerotic plaque was 17%. The MRIs indicated that the abdominal aorta in the experimental group was eccentrically thickened, while the vascular wall of the abdominal aorta in the control group exhibited no abnormality. The intima of the abdominal aorta in the experimental group showed pathological manifestations of unstable atherosclerotic plaque, while that in the control group exhibited no abnormality. This method of modelling is simple to conduct, has a high success rate and requires a short duration, making it an effective animal model of unstable atherosclerotic plaque.

INTRODUCTION

Atherosclerosis (AS) plaque rupture and thrombosis are pathological mechanisms that lead to acute cardiovascular and cerebrovascular events (Rafieian-Kopaei *et al*., 2014) and are important factors in the onset of related diseases that are primary causes of death worldwide (Pagidipati *et al*., 2017). The pathogenesis of AS remains unclear, as it involves a series of steps, including endothelial injury, inflammatory response, metabolic disorders, cell proliferation, foam cell formation and atherosclerotic plaque rupture (Ross, 1999). Among these, the rupture of vulnerable plaque is the main cause of cardiovascular events, with the instability of the plaque largely determining the clinical outcome of the disease. From a clinical perspective, stabilising vulnerable plaques is an important step in controlling the disease; however, at present, there is no relevant treatment.

Unstable plaques have specific histological characteristics, namely a lipid-rich atherosclerotic core, a thin fibrous cap and inflammatory cell infiltration, reduced smooth muscle cell content and remodelling. While great progress has been made in related clinical and rudimentary research, the pathological mechanism of the transformation from unstable to stable plaque remains unclear. The construction of a typical atherosclerotic non-plaque model will be useful when studying the components of atherosclerotic plaque.

High-resolution magnetic resonance imaging (HR-MRI) has been widely used in clinical and elementary research on the non-invasive evaluation of systemic atherosclerotic plaques. Various researchers globally have constructed many animal models for AS plaque and have used MRI to study the attendant aetiology, pathogenesis, complications and treatment (Lee *et al*., 2017). Since HR-MRI involves no ionising radiation and demonstrates high soft-tissue contrasting and spatial resolution, it is a powerful imaging technique for evaluating the morphology, composition and stability of AS plaques by potentially introducing magnetic resonance contrast agents to increase

* Corresponding author: jia_wenxiao@163.com
0030-9923/2022/0001-0001 $ 9.00/0

sensitivity (Nasr *et al.*, 2018). Given that this method presents the optimal non-invasive examination method for evaluating AS plaques (Gao *et al.*, 2016), this study aims to explore a relevant, simple and feasible animal model of unstable atherosclerotic plaque in relation to the abdominal aorta of rabbits and provide a methodological foundation for subsequent studies in this field.

MATERIALS AND METHODS

Study design and high-fat feed

The rationale behind this combined modelling method is as follows. First, although a high-fat di*et al*one can cause arteriosclerosis, this takes longer than a high-fat diet with a balloon injury. A vitamin D injection was also performed to induce the formation of vulnerable plaque. In addition, the intracranial and carotid arteries of New Zealand rabbits are too thin to be observed through the cranial coil. Therefore, the abdominal aorta, which is relatively thick in rabbits, was selected as the site of interest.

Male New Zealand rabbits (age = 3 months, bodyweight = 1.5–2.0 kg) were fed in a single cage at a temperature of 20℃–25℃, a humidity of 50%–60% and light time from 7:00–19:00 daily. The animals were free to drink and eat throughout the experiments, and all the animals were purchased from the animal experiment centre of our university under the following license number: SYXK (new) 2018-0001. The rabbits were randomly divided into the experimental (n= 36) and control (n= 5) groups. The rabbits in the experimental group were given combined interventions, including a balloon injury, a vitamin D injection and a high-fat diet (1% cholesterol, 0.2% bile salt, 20% lard and 10% white sugar; batch no. 201833, Nanjing Shengmin Scientific Research Animal Breeding Institute) once a day for 16 weeks (Phinikaridou *et al.*, 2010). The rabbits in the control group received normal food and no intervention.

Main reagents and instruments

The following materials were used: a dewaxing solution (Solebo, art. YA0031), a phosphate-buffered saline buffer solution (Solebo, art. P1010), haematoxylin (Solebo, art. BL700B), gum (Solebo, art. G8590), an eosin dyeing solution (Solebo, art. G1100), vitamin D (Jilin Huamu Animal Health Products Co., Ltd., art. 170804), heparin (Beijing Solebo Technology Co., Ltd., art. H8060), triglyceride (TG; Nanjing Jiancheng, art. A110-1-1), total cholesterol (TC; Nanjing Jiancheng, art. A111-1-1), high-density lipoprotein (HDL; Nanjing Jiancheng, art. A112-1-1) and low-density lipoprotein (LDL; Nanjing Jiancheng, art. A113-1-11).

The following additional equipment was used: a magnetic resonance scanner (Skyra3.0T, Siemens), a paraffin melting chamber (PM401, LCICA, Germany), a tissue embedding machine (Model 5235, ASKURA, Japan), a drying box (BXH-280, Shanghai Boxun Industrial Co., Ltd.), an optical microscope (DM4000, Leica Microsystems Ltd.), a puncture needle (Shenzhen Infinito Technology Co., Ltd., 8998406), a percutaneous transluminal angioplasty balloon catheter (Henan Zeyuan Medical Equipment Sales Co., Ltd., 26340347), a waterproof constant temperature incubator (Shanghai Boxun Industrial Co., Ltd., B6-270), a vortex mixer (Haimen Qilin Bell Instrument Manufacturing Co., Ltd., GL-88B), a mini centrifuge instrument (Jingqi, MLX-206), a micrometre (Beijing Kaiao Technology Development Co., Ltd., K6600A) and a micro-oscillator (Haimen Qilin Bell Instrument Manufacturing Co., Ltd., BE-3100).

Balloon-induced injury of the intima of the abdominal aorta

Before the procedure for the balloon-induced injury, the rabbits underwent adaptive feeding for a week without fasting (Li *et al.*, 2016). The rabbits were first anaesthetised via an intraperitoneal injection of 10% chloral hydrate (3.5 mL/kg) and then fixed in a supine position on the experimental table (Supplementary Fig. S1A-B). The hair on the abdomen was shaved with an electric razor, and the abdomen was fully exposed before being disinfected with ethanol. A balloon catheter measuring 3.5 × 15 mm was inserted along a 0.014-inch guide wire, and heparin (100 U/kg) was then injected through the auricular vein. The balloon catheter was inserted at around 20 cm, and distilled water was injected at an atmospheric pressure of 14 to fill the balloon and pull it back to the iliac artery three times to cause an intima injury of the abdominal aorta (Supplementary Fig. S2A-D). After withdrawing the balloon catheter, the right distal femoral artery was ligated, the incision was sutured layer-by-layer and specific antibiotics were administered for three consecutive days to prevent infection, with caution applied to minimise the amount of bleeding. One week following the procedure, a bolus of vitamin D (1.5 mL/kg) was injected through an ear vein to promote the formation of an atherosclerotic vulnerable plaque model.

The magnetic resonance scanning process

Magnetic resonance imaging scanning was performed using an HR-MRI platform scanner (Skyra 3.0T; Siemens Healthiness, Erlangen, Germany) with eight-channel cranial coils. The rabbits abdomens were scanned supinely on an MRI table under general anaesthesia and free breathing. Images of the target vessels were obtained using sequential scanning, and the abdominal aortic plaque was

detected using HR-MRI. The plaques were evaluated primarily according to their size (maximum diameter), signal characteristics (whether they were reinforced) and degree of vascular stenosis.

Histopathology and biochemical criteria

Blood was drawn into a tube with heparin anticoagulation from a rabbit's ear vein at the end of the experiment. Frozen centrifugation was used to separate the plasma for 10 min at 6,000 × g and was stored at –80℃ until use. The presence of TC, TG, HDL and LDL in the serum of the rabbits was determined using a biochemical detection kit (Elabscience Biotechnology Co., Ltd, Wuhan, China). Following the instructions of the kit, matching antibodies were diluted in a coating buffer to 1–10 g/mL and then incubated overnight at 4°C before each sample was incubated in a reaction well with 0.1 mL of the antibody solution for 1 h at 37°C. Following this, a further 1 h incubation was carried out with the addition of 0.1 mL of a diluted enzyme-labelled antibody, followed by colour development using a 3, 3', 5, 5'-tetramethylbenzidine substrate solution. To finish, 0.05 mL of sulphuric acid was added, with the optical density monitored using an enzyme-linked immunosorbent assay detector at a wavelength of 450 nm.

Next, the experimental animals were sacrificed via an air injection through the auricular vein, and the entire lower abdominal aorta was resected for histopathological examinations (Fig. 1). Samples of the abdominal aorta were preserved in 4% formaldehyde and embedded in paraffin for histopathology. Then, the embedded tissue was split into 4-μm slices and stained using a hematoxylin and eosin staining kit (Beyotime Institute of Biotechnology, Shanghai, China). Finally, a light microscope was used to scan each segment (Olympus, BX51 microscope, Tokyo, Japan).

Fig. 1. Representative images of the abdominal aorta in the control group and the experimental group. Compared with that in the control group (left panel), the abdominal aorta in the experimental group (right panel) exhibited significant evidence of lipid accumulation and diffuse atherosclerosis.

The lipid in the plaques was quantified using oil red O staining. After being split longitudinally, the abdominal aorta was fixed with 4% paraformaldehyde (PFA). The fixed aortas were pinned to a surface made of black wax, dyed with 0.3% oil red O (Sigma) in 60% isopropanol for 15 min at room temperature, washed with 60% isopropanol for 10 min, and finally, rinsed with water before being preserved in 4% PFA in PBS for imaging. Additionally, serial aorta slices were stained with Masson's Trichrome. The plaque size and number of lipid drops were measured using the Photoshop CS6 software (Adobe Systems, San José, CA). Any plaques that presented macrophage infiltration, a necrotic core, a lipid pool, spotted calcification or intraplaque haemorrhaging were considered vulnerable or unstable (Khan *et al*., 2015).

Statistical analysis

All statistical analyses were performed using SPSS Statistics (v.25.0) (IBM Corp., Silicon Valley, CA, USA). The continuous data were expressed as the mean ± deviation, and the categorical data were expressed as counts (frequency). A student's t-test was used to compare the quantitative data of the experimental and control groups. A two-tailed *P*-value of less than 0.05 was considered to indicate a statistically significant difference.

RESULTS

Survival rate and body weight change

Regarding the 36 rabbits who underwent the procedure, three died due to anaesthesia, two died related to surgical causes, one died due to an excessive contrast agent injection during the HR-MRI and one died during the subsequent feeding, resulting in an overall mortality rate of 17%. There was a significant increase in body weight after the administration of a high-fat diet (3.656 ± 0.1655 kg vs. 2.524 ± 0.1261 kg, $P < 0.0001$).

High-resolution magnetic resonance imaging results

The HR-MRI results indicated that the level of AS in the experimental group ranged from enhancement of the vascular wall following the abdominal aortic enhancement scan at a bilateral renal level to visible eccentric vascular stenosis and localised stenosis (red arrow), while no obvious thickening of the abdominal aortic vascular wall was observed in the control group (Fig. 2). The representative images of the abdominal aorta are shown in (Supplementary Fig. S3A–D).

Pathological results

During general observation, the vascular wall of the control group was soft, elastic and pinkish. The

abdominal aortic vascular wall of the experimental group was significantly thickened, stiff and inelastic, while no abnormal changes were observed in the abdominal aorta of the low-fat control group. Under a light-microscope examination, the lower endothelial layer of the abdominal aorta of the rabbits in the experimental group was observed to be significantly thickened, with lipid depositions and foam cells found on the intima surface, as well as vascular wall fibrous tissue hyperplasia, local vascular wall necrosis and bleeding. In the control group, the intima of the abdominal aorta wall was smooth and exhibited no thickening, lipid deposition or foam cell formation (Figs. 3 and 4). Compared with the control group, the experimental group showed more lipid drops in the cross-sectional images of oil red O staining (9.778 ± 2.224 vs 2.778 ± 1.202, $P < 0.001$; Supplementary Fig. S4A–B). In addition, the experimental group demonstrated a significantly higher fibrosis area than the control group (11.06 ± 1.444 vs 1.303 ± 0.578 mm^2, $P < 0.001$; Supplementary Fig. S4C–D).

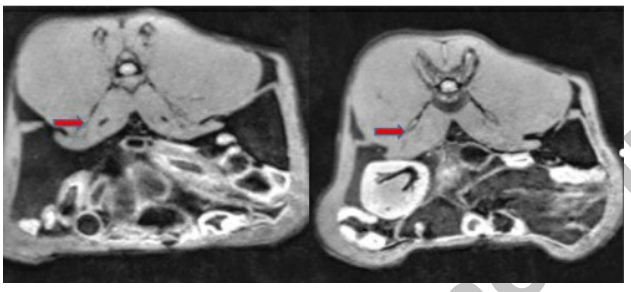

Fig. 2. Cross-sectional images of high-resolution MR examination in the experimental group. The HR-MRI images showed an enhancement of the vascular wall following the abdominal aortic enhancement scan at a bilateral renal level to visible eccentric vascular stenosis and localized stenosis (red arrow).

Serum lipid test results

As shown in Table I, compared to the control group, the TC (3.26 ± 0.41 vs 25.54 ± 0.38), TG (1.25 ± 0.04 vs 3.08 ± 0.12) and LDL (2.18 ± 0.46 vs 20.38 ± 0.36) in the experimental group significantly increased ($P < 0.001$ for all), while the HDL content significantly decreased (0.45 ± 0.24 vs 1.54 ± 0.27; $P < 0.001$).

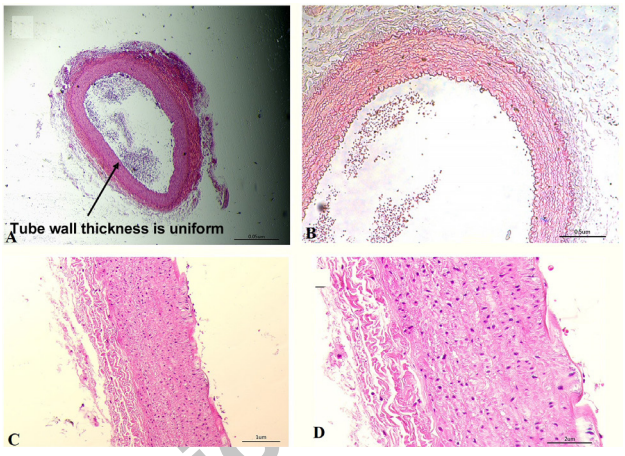

Fig. 3. Histological images of the abdominal aorta in the control group: A, abdominal aorta ×10; B, abdominal aorta ×100; C, abdominal aorta ×200; D, abdominal aorta ×400.

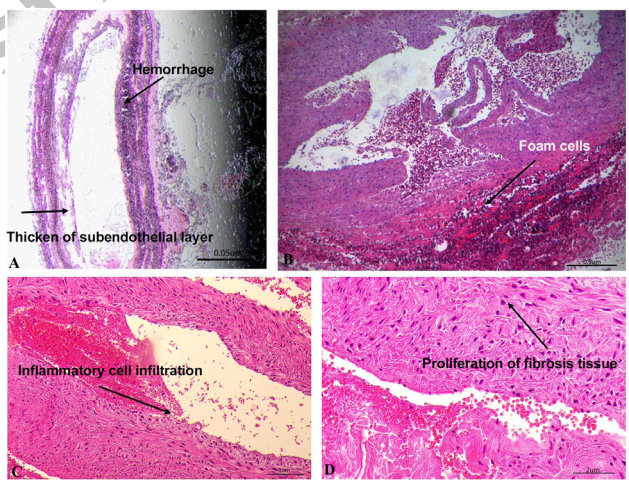

Fig. 4. Histological images of the abdominal aorta in the case group: A, abdominal aorta ×10; B, abdominal aorta ×100; C, abdominal aorta ×200; D, abdominal aorta ×400.

Table I. Comparison of serum lipid content between the low-fat control group and the model group.

Group	TG	TC	HDL	LDL
Low-fat control group	1.25 ± 0.04	3.26 ± 0.41	0.45 ± 0.24	2.18 ± 0.46
Model group	3.08 ± 0.12	25.54 ± 0.38	1.54 ± 0.27	20.38 ± 0.36
t	22.28	11.17	9.933	14.68
P	0.0001	0.0001	0.0001	0.0001

Values are presented as mean±standard deviation. HDL, high-density lipoprotein; LDL, low-density lipoprotein; TC, total cholesterol; TG, triglycerides.

DISCUSSION

In this study, a method of constructing a vulnerable atherosclerotic plaque model in the abdominal aorta of rabbits was evaluated in terms of efficacy and feasibility. The main findings were as follows: (1) the mortality rate of the New Zealand rabbits that underwent the model construction was approximately 17%; (2) the HR-MRI results revealed an eccentric thickening pattern in the abdominal aorta of the experimental group, which was not observed in the control group; (3) in the pathological examinations, the intima of the abdominal aorta in the experimental group exhibited typical features of unstable atherosclerotic plaque, while the control group exhibited only normal manifestations. The method demonstrated ease of operation, a high success rate and a relatively low modelling time, providing a methodological foundation for further studies in this field.

A balloon operation was performed to damage the intima of the abdominal aorta. No single animal model can exhibit all the features of human AS. As a result, many different animals have been used to illustrate different aspects of AS. At present, the main animal models that are generally used in studies are mouse and rabbit models, followed by pig and non-human primates. Each model has its advantages and limitations. Among those used to date, rabbits are one of the preferred models for investigating lipoprotein metabolism and AS. Lipid accumulation is a key event in the formation of atherosclerotic lesions. New Zealand rabbits were chosen for the animal model since their lipoprotein metabolism and vascular structure are highly similar to those of humans and because they are highly sensitive to high-fat feed and are thus often selected for AS plaque models (Fan *et al*., 2015). The pathological properties of the AS plaques that formed were also highly similar to those found in humans (Rekhter, 2002). Rabbits have the advantages of a moderate size, convenient feeding regime, convenient blood collection/examination and low cost (Fang *et al*., 2009), and the morphology of rabbit plaque is similar to that of human plaque. Therefore, this type of model presents an ideal experimental research model for studying human AS non-plaque lesions.

Masley *et al*. (2003) fed rabbits a high-fat diet in a study conducted in 1931, thereby successfully constructing the first rabbit model of AS plaque for human AS-related research. Elsewhere, Xu *et al*. (2020) fed rabbits a high-fat diet for 12 weeks and successfully constructed a carotid AS plaque model, with the authors using ultrasound, HR-MRI and positron emission tomography/computer tomography techniques to evaluate the carotid artery diagnostic effect of the model. Furthermore, based on the pathogenesis of AS, an AS model can be constructed based on the autoimmune theory (Spartalis *et al*., 2020). Tang *et al*. (2016) injected foetal bovine serum albumin intramuscularly for a vascular immune injury and then fed the experimental animals a high-fat diet, thereby successfully constructing a rabbit AS plaque model.

A vascular examination via the bone window is often not achievable when evaluating vascular plaques by ultrasound, particularly when it comes to human cerebrovascular tests. It should be noted that recent research found HR-MRI to be more accurate in diagnosing carotid atherosclerotic plaques than an ultrasound (Gao *et al*., 2010). The main benefit of HR-MRI is the ability to collect and combine multiple contrast images, including both bright and black blood, to distinguish the tissue composition within the atherosclerotic vessel wall. Compared with a low-resolution ultrasound, the HR-MRI technique can reveal the presence of AS plaque with a high resolution in terms of morphology, composition (e.g., lipid core, calcification and intraplaque haemorrhage), surface (e.g., thrombus) and vascular lumen (Choi *et al*., 2015), with the method demonstrating high sensitivity and specificity. The technique can be used to analyse the composition and classification of plaque to estimate the stability of the plaque and ensure the early detection of vulnerable plaque (Xu *et al*., 2014). This approach also allows for a non-invasive evaluation of AS plaque and a powerful examination of the attendant morphology, composition and stability.

Although imaging techniques can detect anatomical parameters associated with vulnerable plaques, they have not successfully determined which plaques are most likely to result in a cardiovascular incident. Plaque disruption cannot be controlled experimentally, making studies of human atherothrombosis extremely difficult. The rabbit model in the current study has the benefit of being able to mimic most forms of human plaque in the rabbit aorta and allows for the experimental control of plaque disintegration. It is anticipated that this model's approach will be helpful for the study of vulnerable plaques and ultimately facilitate the translation of basic research findings into clinical applications. It should be noted that the lack of intraplaque bleeding and plaque calcification is a drawback of this rabbit model. Although both of these features could be achieved in some settings, there is still a degree of distance between this model and a human model of vulnerable plaque.

Atherosclerosis plaque is the result of various factors, and AS that is produced due to a single factor may significantly differ from that observed in humans. Therefore, the construction of AS models using composite methods has received increasing attention among researchers (Wang *et al*., 2015). In this study, a rabbit model reflecting unstable atherosclerotic plaque of the

abdominal aorta was constructed using the following three approaches: high-fat feeding, abdominal aortic balloon injury and vitamin D injection. In addition, studies have shown that hyperlipidaemia activated the inflammatory immune response in vivo and damaged the intima of blood vessels, thereby presenting the initiating factor for the formation of AS (Zhao *et al*., 2018; Liang *et al*., 2018). Blood monocytes and macrophages enter the tunica intima in response to endothelial lesions, where they collect cholesterol-rich low-density lipoprotein particles from the bloodstream and create atherosclerotic plaques (Skålén *et al*., 2002; Luo *et al*., 2020). High levels of LDL significantly speed up the development of AS, which generally takes years or even decades to develop. The biochemical indicators in the present study indicated that, compared to the control group, the amount of TC, TG and LDL increased significantly in the experimental group, but the HDL content was higher in the control than in the experimental group. In this study, pathological sections of all the rabbits abdominal aortas were created, and the subsequent haematoxylin and eosin staining confirmed lipid deposition and plaque formation in the medial membrane of the abdominal aorta of both the experimental and control groups, which further confirmed that the experimental group presented a better AS vulnerable plaque model (Khan *et al*., 2015).

This study had several limitations. First, the formation of human atherosclerotic plaque involves a long and complex process, and this study was limited in terms of the life span of the animals, which died due to various causes. The overall survival rate of the experimental rabbits at the end of 16 weeks was 83%. Second, while the process of the observation of AS plaque via HR-MRI to evaluate the level of abdominal aorta plaque vulnerability entailed 16 weeks for pathological evaluation, HR-MRI is not as effective as ultrasonic imaging; the author aims to adopt the latter method in subsequent research to improve the reliability of the experimental results. Third, we did not measure the amount of oxidised LDL in serum, which is one of the main causes of vulnerable plaque rupture. However, the HR-MRI and pathological staining could directly reflect the anatomy of vulnerable plaque and verify the feasibility of this modelling method.

CONCLUSION

In conclusion, high-fat feeding combined with an abdominal aortic balloon injury and vitamin D injection was used to establish an ideal rabbit model of abdominal aortic unstable atherosclerotic plaque, thereby providing a good experimental basis for the study and treatment of human atherosclerotic vulnerable plaque.

Ethics approval and consent to participate

This study was conducted in accordance with the Declaration of Helsinki and approved by the ethics committee of Kangzhirui animal experiment center (XJKZR20201016).

Availability of data and material

The datasets used or analyzed during the current study are available from the corresponding author on reasonable request.

Funding

National Natural Science Foundation of China Regional Science Fund Project: 81860301.

Supplementary material

There is supplementary material associated with this article. Access the material online at: https://dx.doi.org/10.17582/journal.pjz/20220926100938

Statement of conflict of interest

The authors have declared no conflict of interest.

REFERENCES

Choi, Y.J., Jung, S.C. and Lee, D.H., 2015. Vessel wall imaging of the intracranial and cervical carotid arteries. *J. Stroke*, **17**: 238-255. https://doi.org/10.5853/jos.2015.17.3.238

Fan, J., Kitajima, S., Watanabe, T., Xu, J., Zhang, J., Liu, E. and Chen, Y.E., 2015. Rabbit models for the study of human atherosclerosis from pathophysiological mechanisms to translational medicine. *Pharmacol. Ther*., **146**: 104-119. https://doi.org/10.1016/j.pharmthera.2014.09.009

Fang, S.M., Zhang, Q.H. and Jiang, Z.X., 2009. Developing a novel rabbit model of atherosclerotic plaque rupture and thrombosis by cold-induced endothelial injury. *J. Biomed. Sci*., **16**: 39. https://doi.org/10.1186/1423-0127-16-39

Gao, T.L., Yu, W. and Zhang, Z., 2010. The comparative study of high-resolution MRI and ultrasound in assessment of carotid atherosclerosis. *Chin. J. Geriatr. Heart Brain Vessel Dis*., **12**: 915–917.

Gao, Z., Ma, T., Zhao, E., Docter, D., Yang, W., Stauber, R.H. and Gao, M., 2016. Small is smarter: Nano MRI contrast agents, Advantages and Recent Achievements. *Small*, **12**: 556-576. https://doi.org/10.1002/smll.201502309

Khan, R., Spagnoli, V., Tardif, J.C. and L'Allier, P.L., 2015. Novel anti-inflammatory therapies for the treatment of atherosclerosis. *Atherosclerosis*, **240**: 497-509. https://doi.org/10.1016/j.

atherosclerosis.2015.04.783

Lee, Y.T., Lin, H.Y., Chan, Y.W., Li, K.H., Ling To, O.T., Yan, B.P., Liu, T., Li, G.P., Wong, W.T., Keung, W. and Tse, G., 2017. Mouse models of atherosclerosis: a historical perspective and recent advances. *Lipids Hlth. Dis*., **16**: 12. https://doi.org/10.1186/s12944-016-0402-5

Li, Z., Wang, L., Hu, X., Zhang, P., Chen, Y., Liu, X., Xu, M., Zhang, Y. and Zhang, M., 2016. Effect of rosuvastatin on atherosclerotic plaque stability: An intravascular ultrasound elastography study. *Atherosclerosis*, **248**: 27-35. https://doi.org/10.1016/j.atherosclerosis.2016.02.028

Liang, C., Wang, Q.S., Yang, X., Niu, N., Hu, Q.Q., Zhang, B.L., Wu, M.M., Yu, C.J., Chen, X., Song, B.L., Zhang, Z.R. and Ma, H.P., 2018. Oxidized low-density lipoprotein stimulates epithelial sodium channels in endothelial cells of mouse thoracic aorta. *Br. J. Pharmacol*., **175**: 1318-1328. https://doi.org/10.1111/bph.13853

Luo, J., Yang, H. and Song, B.L., 2020. Mechanisms and regulation of cholesterol homeostasis. *Nat. Rev. Mol. Cell Biol*., **21**: 225-245. https://doi.org/10.1038/s41580-019-0190-7

Masley, S., Kenney, J.J. and Novick, J.S., 2003. Optimal diets to prevent heart disease. *JAMA*, **289**: 1510. https://doi.org/10.1001/jama.289.12.1510-a

Nasr, S.H., Tonson, A., El-Dakdouki, M.H., Zhu, D.C., Agnew, D., Wiseman, R., Qian C. and Huang X., 2018. Effects of nanoprobe morphology on cellular binding and inflammatory responses: Hyaluronan-conjugated magnetic nanoworms for magnetic resonance imaging of atherosclerotic plaques. *ACS appl. Mater. Interfaces*, **10**: 11495-11507. https://doi.org/10.1021/acsami.7b19708

Pagidipati, N.J., Hess, C.N., Clare, R.M., Akerblom, A., Tricoci, P., Wojdyla, D., keenan, R.T., James, S., Held, C., Mahaffey, K.W., Klein, A.B., Wallentin, L. and Roe, M.T., 2017. An examination of the relationship between serum uric acid level, a clinical history of gout, and cardiovascular outcomes among patients with acute coronary syndrome. *Am. Heart J*., **187**: 53-61. https://doi.org/10.1016/j.ahj.2017.02.023

Phinikaridou, A., Ruberg, F.L., Hallock, K.J., Qiao, Y., Hua, N., Viereck, J. and Hamilton, J.A., 2010. *In vivo* detection of vulnerable atherosclerotic plaque by MRI in a rabbit model. *Circ. Cardiovasc. Imaging*, **3**: 323-332. https://doi.org/10.1161/CIRCIMAGING.109.918524

Rafieian-Kopaei, M., Setorki, M., Doudi, M., Baradaran, A. and Nasri, H., 2014. Atherosclerosis: Process, indicators, risk factors and new hopes. *Int. J. Prev. Med*., **5**: 927-946.

Rekhter, M.D., 2002. How to evaluate plaque vulnerability in animal models of atherosclerosis? *Cardiovasc. Res*., **54**: 36-41. https://doi.org/10.1016/S0008-6363(01)00537-5

Ross, R., 1999. Atherosclerosis an inflammatory disease. *N. Engl. J. Med*., **340**: 115-126. https://doi.org/10.1056/NEJM199901143400207

Skålén, K., Gustafsson, M., Rydberg, E.K., Hulten, L.M., Wiklund, O., Innerarity, T.L. and Boren, J., 2002. Subendothelial retention of atherogenic lipoproteins in early atherosclerosis. *Nature*, **417**: 750-754. https://doi.org/10.1038/nature00804

Spartalis, M., Spartalis, E., Athanasiou, A., Paschou, S.A., Kontogiannis, C., Georgiopoulos, G., Iliopoulos, D.C. and Voudris, V., 2020. The role of the endothelium in premature atherosclerosis: Molecular mechanisms. *Curr. Med. Chem*., **27**: 1041-1051. https://doi.org/10.2174/0929867326666190911141951

Tang, X., Yang, S., Gou, B., Wu, S., Jiang, L. and Liu, P., 2016. High fat diet combined with immune injury to establish rabbit atherosclerosis model and evaluation. *China Med. Her*., **13**: 21-24.

Wang, Q., Huo, L., He, J., Ding, W., Su, H., Tian, D., Welch, C., Hammock, B.D., Ai, D. and Zhu, Y., 2015. Soluble epoxide hydrolase is involved in the development of atherosclerosis and arterial neointima formation by regulating smooth muscle cell migration. *Am. J. Physiol. Heart Circ. Physiol*., **309**: H1894-903. https://doi.org/10.1152/ajpheart.00289.2015

Xu, L., Wang, R., Liu, H., Wang, J., Liang, W., Mang, J. and Xu, Z., 2020. Comparison of the diagnostic performances of ultrasound, high-resolution magnetic resonance imaging, and positron emission tomography/computed tomography in a rabbit carotid vulnerable plaque atherosclerosis model. *J. Ultrasound Med*., **39**: 2201-2209. https://doi.org/10.1002/jum.15331

Xu, W.H., Li, M.L., Niu, J.W., Feng, F., Jin, Z.Y. and Gao, S., 2014. Intracranial artery atherosclerosis and lumen dilation in cerebral small-vessel diseases: A high-resolution MRI Study. *CNS Neurosci. Ther*., **20**: 364-367. https://doi.org/10.1111/cns.12224

Zhao, X., Zhang, H.W., Xu, R.X., Guo, Y.L., Zhu, C.G., Wu, N.Q., Gao, Y. and Li, J.J., 2018. Oxidized-LDL is a useful marker for predicting the very early coronary artery disease and cardiovascular outcomes. *Per Med*., **15**: 521-529. https://doi.org/10.2217/pme-2018-0046

Pakistan J. Zool., pp 1-7, 2022. **DOI**: https://dx.doi.org/10.17582/journal.pjz/20220926100938

Supplementary Material

The Establishment and Evaluation of an Atherosclerotic Vulnerable Plaque Model Involving New Zealand Rabbits

Wenxiao Jia[1]*, Yilinuer Yilihamu[1], Yunling Wang[1], Shuang Ding[1], Dilinuerkezi Aihemaiti[1], Hanjiaerbieke Kukun[1] and Yanhui Ning[2]

[1]Department of Radiology, First Affiliated Hospital of Xinjiang Medical University, Urumqi 830011, China
[2]Xinjiang Kangzhirui Biomedical Technology Service Company, Urumqi 830001, China

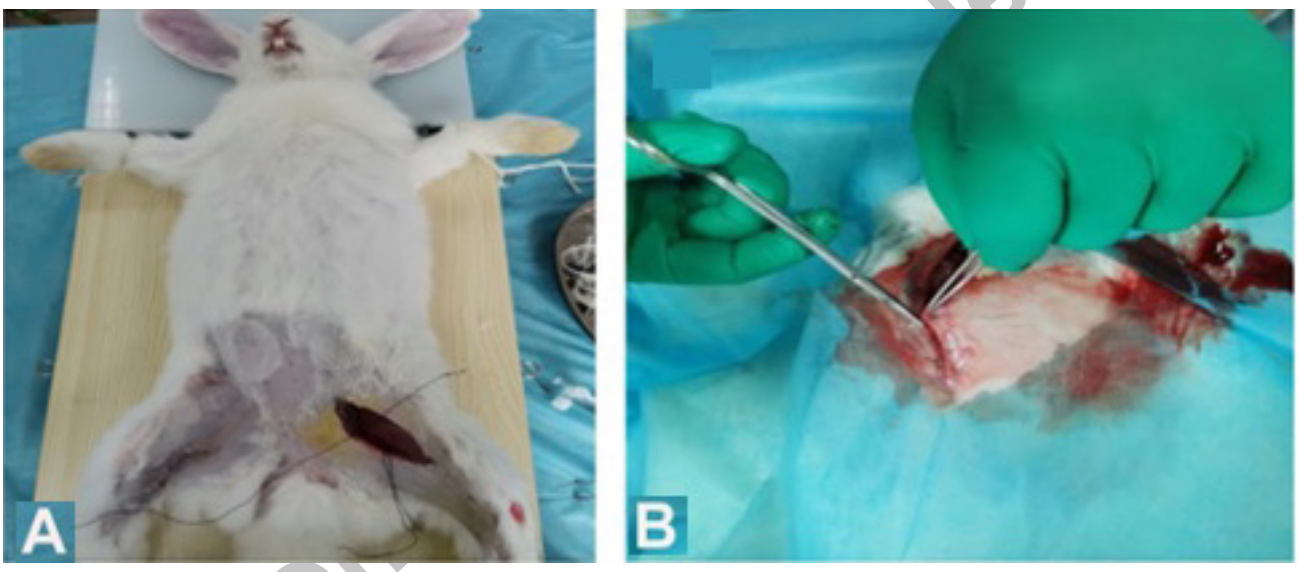

Supplementary Fig. S1. Representative images of the procedure in the right femoral artery. (A) The animals were anesthetized by intraperitoneal injection of 10% chloral hydrate (3.5 ml/kg) and fixed on the experimental table in supine position. The skin was prepared and sterilized. The skin was cut distally along the leg in the medial groin, and the incision was 5-6 cm to separate the right femoral artery. (B) After the balloon catheter was withdrawn, the right distal femoral artery was ligated, and the incision was sutured layer by layer.

* *Corresponding author: jia_wenxiao@163.com*
0030-9923/2022/0001-0001 $ 9.00/0

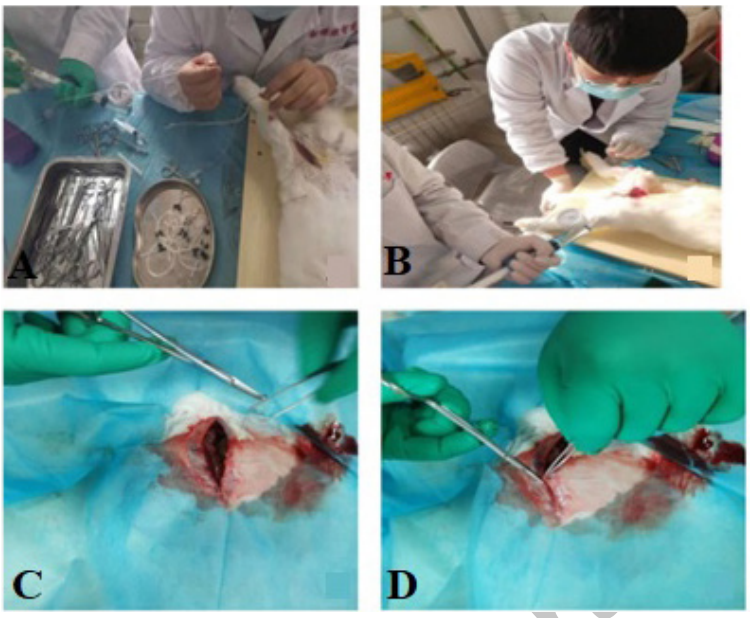

Supplementary Fig. S2. Representative images of the modeling procedure. (A-B) The catheter is introduced into the right femoral artery and balloon is inflated to induce the vascular injury; (C-D) The distal femoral artery and superficial skin are ligated.

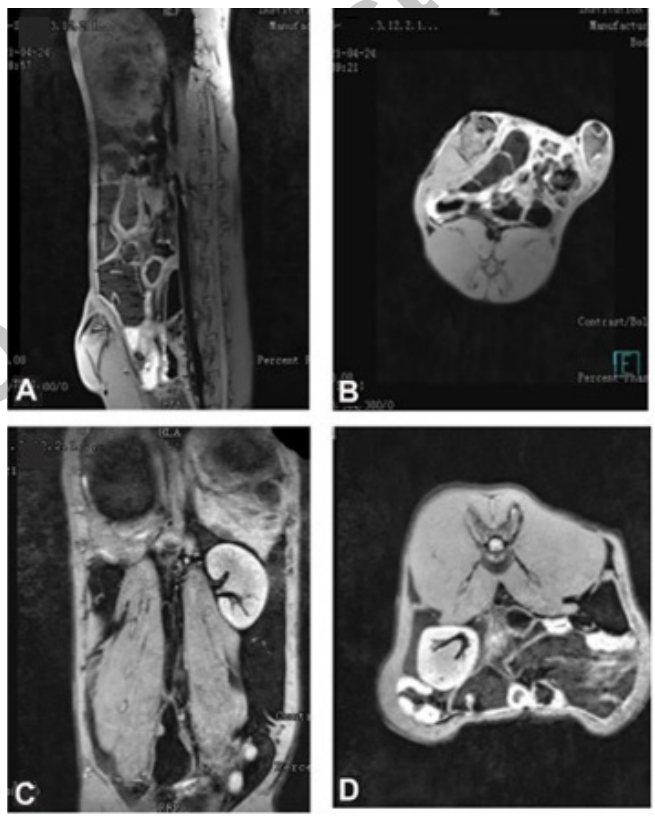

Supplementary Fig. S3. HR-MRI images of the abdominal aorta among normal and atherosclerotic experimental groups. (A-B) Normal abdominal aortic vessel wall; (C-D) Abdominal aorta in a rabbit model of atherosclerosis. Eccentric thickening is shown by HR-MRI in a rabbit model of atherosclerosis. HR-MRI: high resolution magnetic resonance imaging.

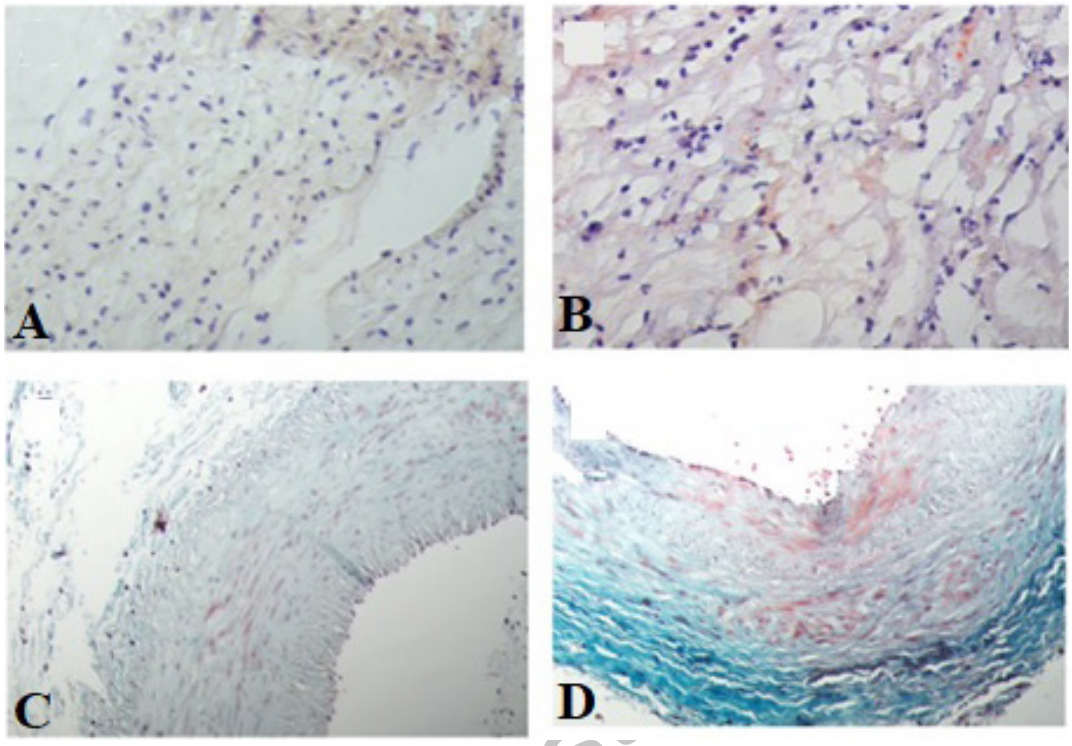

Supplementary Fig. S4. Pathological cross-sectional images of the abdominal aorta in the two groups. (A) Oil red O staining in the control group (40X); (B) Oil red O staining in the high-fat experimental group (40X); (C) Masson staining of blood vessel wall in the control group; (D) Masson staining of blood vessel wall in the high-fat experimental group.